



HAL
open science

Generic tests of the existence of the gravitational dipole radiation and the variation of the gravitational constant

K. Lazaridis, N. Wex, A. Jessner, M. Kramer, B.W. Stappers, G.H. Janssen, G. Desvignes, M.B. Purver, Ismaël Cognard, Gilles Theureau, et al.

► To cite this version:

K. Lazaridis, N. Wex, A. Jessner, M. Kramer, B.W. Stappers, et al.. Generic tests of the existence of the gravitational dipole radiation and the variation of the gravitational constant. *Monthly Notices of the Royal Astronomical Society*, 2009, 400 (2), pp.805-814. 10.1111/j.1365-2966.2009.15481.x . insu-02778975

HAL Id: insu-02778975

<https://insu.hal.science/insu-02778975>

Submitted on 4 Jun 2020

HAL is a multi-disciplinary open access archive for the deposit and dissemination of scientific research documents, whether they are published or not. The documents may come from teaching and research institutions in France or abroad, or from public or private research centers.

L'archive ouverte pluridisciplinaire **HAL**, est destinée au dépôt et à la diffusion de documents scientifiques de niveau recherche, publiés ou non, émanant des établissements d'enseignement et de recherche français ou étrangers, des laboratoires publics ou privés.

Generic tests of the existence of the gravitational dipole radiation and the variation of the gravitational constant

K. Lazaridis,^{1*}† N. Wex,¹ A. Jessner,¹ M. Kramer,^{1,2} B. W. Stappers,^{2,3} G. H. Janssen,⁴ G. Desvignes,⁵ M. B. Purver,² I. Cognard,⁵ G. Theureau,⁵ A. G. Lyne,² C. A. Jordan² and J. A. Zensus¹

¹Max-Planck-Institut für Radioastronomie, Auf dem Hügel 69, 53121, Bonn, Germany

²University of Manchester, Jodrell Bank Centre for Astrophysics, Alan Turing Building, Manchester M13 9PL

³Stichting ASTRON, Postbus 2, 7990 AA, Dwingeloo, the Netherlands

⁴Astronomical Institute Anton Pannekoek, University of Amsterdam, Postbus 94249, 1090 GE Amsterdam, the Netherlands

⁵Laboratoire de Physique et Chimie de l'Environnement, CNRS, 3A Avenue de la Recherche Scientifique, 45071 Orléans Cedex 2, France

Accepted 2009 August 2. Received 2009 July 30; in original form 2009 July 10

ABSTRACT

We present results from the high-precision timing analysis of the pulsar-white dwarf (WD) binary PSR J1012+5307 using 15 years of multitelescope data. Observations were performed regularly by the European Pulsar Timing Array (EPTA) network, consisting of Effelsberg, Jodrell Bank, Westerbork and Nançay. All the timing parameters have been improved from the previously published values, most by an order of magnitude. In addition, a parallax measurement of $\pi = 1.2(3)$ mas is obtained for the first time for PSR J1012+5307, being consistent with the optical estimation from the WD companion. Combining improved 3D velocity information and models for the Galactic potential, the complete evolutionary Galactic path of the system is obtained. A new intrinsic eccentricity upper limit of $e < 8.4 \times 10^{-7}$ is acquired, one of the smallest calculated for a binary system and a measurement of the variation of the projected semimajor axis also constrains the system's orbital orientation for the first time. It is shown that PSR J1012+5307 is an ideal laboratory for testing alternative theories of gravity. The measurement of the change of the orbital period of the system of $\dot{P}_b = 5(1) \times 10^{-14}$ is used to set an upper limit on the dipole gravitational wave emission that is valid for a wide class of alternative theories of gravity. Moreover, it is shown that in combination with other binary pulsars PSR J1012+5307 is an ideal system to provide self-consistent, generic limits, based only on millisecond pulsar data, for the dipole radiation and the variation of the gravitational constant \dot{G} .

Key words: binaries: general – pulsars: general – pulsars: individual: PSR J1012+5307.

1 INTRODUCTION

PSR J1012+5307 is a 5.3-ms pulsar in a binary system with orbital period of 14.5 h and a low-mass companion (Nicastro et al. 1995). It was discovered during a survey for short-period pulsars with the 76-m Lovell radio telescope at Jodrell Bank. Lorimer et al. (1995) reported optical observations revealing an optical counterpart within 0.2 ± 0.5 arcsec of the pulsar timing position being consistent with a helium white dwarf (WD) companion.

The optical observations of the WD companion provide unique information about the evolution of the binary system and the radio pulsar itself, such as comparing the cooling age of the companion with the spin-down age of the pulsar (Lorimer et al. 1995; Driebe et al. 1998; Ergma, Sarna & Gerskevits-Antipova 2001).

Using the NE2001 model for the Galactic distribution of free electrons (Cordes & Lazio 2002) and the pulsar's dispersion measure (DM) of $9 \text{ cm}^{-3} \text{ pc}$ (Nicastro et al. 1995) a distance of ~ 410 pc is derived. In contrast, Callanan, Garnavich & Koester (1998) compared the measured optical luminosity of the WD to the value expected from WD models and calculated a distance of $d = 840 \pm 90$ pc. In addition they measured, by the Doppler shift of the measured H spectrum of the companion, a radial velocity component of $44 \pm 8 \text{ km s}^{-1}$ relative to the Solar system barycentre (SSB). From the radial velocity and the orbital parameters of the system, the mass ratio

*Member of the International Max Planck Research School (IMPRS) for Astronomy and Astrophysics at the Universities of Bonn and Cologne.
†E-mail: klazarid@mpifr-bonn.mpg.de

of the pulsar and its companion was measured to be $q = m_p/m_c = 10.5 \pm 0.5$. Finally, by fitting the spectrum of the WD to a grid of DA (hydrogen dominated) model atmospheres, they derived a companion mass of $m_c = 0.16 \pm 0.02 M_\odot$, a pulsar mass of $m_p = 1.64 \pm 0.22 M_\odot$ and an orbital inclination angle of $i = 52^\circ \pm 4^\circ$.

Lange et al. (2001) presented the most complete precision timing analysis of PSR J1012+5307 using 4 yr of timing data from the Effelsberg 100 m radio telescope and 7 yr from the 76 m Lovell telescope. Using their low eccentricity binary model ELL1 and combining the timing measurements with the results from the optical observations they derived the full 3D velocity information for the system. Furthermore, after correcting for Doppler effects, they derived the intrinsic spin parameters of the pulsar and a characteristic age of 8.6 ± 1.9 Gyr which is consistent with the WD age from the optical estimates. In addition, after calculating upper limits for an extremely low orbital eccentricity, they discussed evolutionary scenarios for the binary system but also presented tests and limits of alternative theories of gravitation. Finally, they discussed the prospects of future measurements of Post-Keplerian (PK) parameters which can contribute to the description of the orientation of the system and the calculation of stringent limits for the effective coupling strength of the scalar field to the pulsar.

In this paper, we revisit PSR J1012+5307 with seven more years of high-precision timing data and combined data sets from the European Pulsar Timing Array (EPTA) telescopes consisting of the 100 m Effelsberg radio telescope of the Max-Planck-Institute for Radioastronomy, Germany, the 76-m Lovell radio telescope at Jodrell Bank observatory of the University of Manchester, UK, the 94-m equivalent Westerbork Synthesis Radio Telescope (WSRT), the Netherlands and the 94-m equivalent Nançay decimetric Radio Telescope (NRT), France. After a short description of the timing procedure and the technique of combining our multitelescope data, we present the updated measurements of the astrometric, spin and binary parameters for the system. Specifically, we show the improvement in all the timing parameters and in the orbital eccentricity limit and in addition the value for the first time for PSR J1012+5307 of the timing parallax. Furthermore, we obtain a value for the orbital period variation, in agreement with the prediction of (Lange et al. 2001), from which we test different theories of gravitation and give one of the tightest bounds on a Parametrized Post-Newtonian parameter. Finally, we present how the timing measurement of the change of the projected semimajor axis can complete the picture of the orientation of the binary system.

2 OBSERVATIONS

2.1 Effelsberg

PSR J1012+5307 was observed regularly with the Effelsberg 100-m radio telescope since 1996 October with typical observing times of 5–15 min in three consecutive scans. Monthly observations were performed at 1400 MHz using the primary focus cooled High Electron Mobility Transistor (HEMT) receiver. It has a typical system temperature of 25 K and an antenna gain of 1.5 KJy^{-1} . In order to monitor DM variations, it was also observed irregularly until 2006 August and monthly thereafter, at 2700 MHz. At these frequencies, a cooled HEMT receiver located at the secondary focus was used which has a system temperature of 25 K. Finally, it was occasionally observed at 860 MHz using an uncooled HEMT receiver, located at the primary focus, with a typical system temperature of 60 K. The Effelsberg–Berkeley Pulsar Processor was used for coherent on-line dedispersion of the signal from the left-hand circular (LHC)

and right-hand circular (RHC) polarizations. It has 32 channels for both polarizations spread across bandwidths of 40, 100 and 80 MHz at 860, 1400 and 2700 MHz, respectively (Backer et al. 1997). The output signals of each channel were fed into dedisperser boards for coherent on-line dedispersion and were synchronously folded with the topocentric period.

Each time of arrival (TOA) was obtained by cross-correlation of the profile with a synthetic template, which was constructed out of 12 Gaussian components fitted to a high signal-to-noise ratio standard profile (Kramer et al. 1998, 1999). The TOAs were locally time stamped using a H-maser clock at the observatory. They were converted to Coordinated Universal Time (UTC) using the Global Positioning System (GPS) maser offset values measured at the observatory, and the GPS to UTC corrections were made from the Bureau International des Poids et Mesures (BIPM¹).

2.2 Jodrell bank

PSR J1012+5307 has been observed with the Lovell radio telescope 2–3 times per month since 1993, at three different frequencies. It is continuously observed at 1400 MHz and at 410 and 606 MHz, it was observed until 1997 and 1999, respectively. All the receivers are cryogenically cooled with system temperatures of 25, 50 and 35, respectively, and their left-hand circular (LHC) and right-hand circular (RHC) polarization signals are detected and incoherently dedispersed in a $2 \times 32 \times 0.0312$ MHz filter bank at 410 MHz, in a $2 \times 6 \times 0.1250$ MHz filter bank at 606 MHz and in a $2 \times 32 \times 1$ MHz filter bank at 1400 MHz. The signals are synchronously folded at the topocentric pulsar period and finally copied to a disc.

Each TOA was obtained by cross-correlation of the profile with a standard template, generated by the summation of high-S/N profiles. The TOAs were transferred to GPS from a H-maser and the time stamp was derived as for Effelsberg.

2.3 Westerbork

PSR J1012+5307 was observed monthly using the WSRT with Pulsar Machine-I (Voûte et al. 2002). We used three observing frequencies: observations at centre frequencies of 1380 and 350 MHz were carried out monthly from August 1999, and the pulsar was observed occasionally at a centre frequency of 840 MHz from 2000 until 2002. The system temperatures were 27, 120 and 75 K, respectively and most observations were 30 min long. The WSRT observations used a bandwidth of 8×10 MHz for observations at 840 and 1380 MHz, and after September 2006 the eight bands were spread out over a total observing bandwidth of 160 MHz for the 1380 MHz observations. The observations at the low-frequency setup used only two bands of 10 MHz, either centred at 328 and 382 MHz or 323 and 367 MHz. For the observations taken at 1380 or 840 MHz, we used 64 frequency channels per 10 MHz band, and the observations at the low frequencies used 256 frequency channels per 10 MHz band.

For each observation, the data were dedispersed and folded off-line. Integration over frequency and time resulted in one single profile for each observation. Each profile was cross-correlated with a standard template, generated by the summation of high-S/N profiles, so finally only one TOA was computed for each observation. The TOAs were transferred to GPS from a H-maser clock and the time stamp was derived as for Effelsberg.

¹ <http://www.bipm.org>

Table 1. Properties of the individual telescope data sets.

Properties	Effelsberg	Jodrell Bank	Westerbork	Nançay
Number of TOAs	1972	600	234	86
Time span (MJD)	50371–54717	49221–54688	51389–54638	53309–54587
rms of individual set(μ s)	2.7	8.6	2.9	1.9
Observed frequencies (MHz)	860, 1400, 2700	410, 606, 1400	330, 370, 840, 1380	1400

2.4 Nançay

PSR J1012+5307 was observed roughly every 3–4 weeks with the Nançay Radio Telescope (NRT) since late 2004. The Nançay Radio Telescope is equivalent to a 94-m dish, with a gain of 1.4 K Jy^{-1} and a minimal system temperature of 35 K at 1.4 GHz in the direction of the pulsar. With the Berkeley–Orleans–Nançay (BON) coherent dedispersor, in the period covered by the observations, a 64-MHz band centred on 1398 MHz is split into sixteen 4-MHz channels and coherently dedispersed using a PC-cluster, with typical integration times of 1 h. The Nançay data are recorded on a UTC (GPS) time-scale marked at the analogue to digital converter by a Thunderbolt receiver (Trimble Inc.). Differences between UTC and UTC (GPS) are less than 10 ns and therefore no laboratory clock corrections are needed. A single TOA was calculated from a cross-correlation with a pulse template for each observation of 1 h.

2.5 Multitelescope precision timing

Combing the EPTA multitelescope data sets is not a trivial process. The main technique for achieving the optimal combination of the data sets is presented by Janssen et al. (2008). In general, using different data sets from different telescopes and obtained at different frequencies requires extra corrections, apart from the usual one of the transformation of all the individual telescope arrival times to arrival times in the International Atomic Time at the SSB. The extra corrections needed are usually constant time offsets between different data sets of residuals. These offsets derive from differences in the procedure of calculating the TOAs at each telescope, specifically differences in the templates. The timing software package TEMPO² can fit for these time offsets or ‘jumps’. In the current work, seven of these jumps need to be fitted corresponding not only to the telescopes but also to the different frequencies used. Normally, three ‘jumps’, one for each telescope, would be sufficient. However, the TOAs at different frequencies are usually calculated by different templates, which might not be aligned optimally. In the current case, this occurs for Effelsberg and Westerbork TOAs. In Table 1, the properties of the individual data sets are presented.

The combination of the EPTA data sets has many advantages (Janssen et al. 2008). The need for continuous multifrequency TOAs for precise measurement of the DM and monitoring of the DM variations was successfully accomplished. Most important the combination of the high-quality data from Effelsberg, Nançay, WSRT with the long-time span data of Jodrell (and Effelsberg) provides us with a 15-yr data set of TOAs with no significant time gaps. Using all these EPTA data sets, we improve and measure all the astrometric, spin and binary parameters of PSR J1012+5307 presented in the first column of Table 2. As a comparison, in the second column the measured parameters of only the current Effelsberg set is shown and

in the third the Effelsberg measurements from Lange et al. (2001). From Table 2, it is clear that the EPTA provides the most accurate error estimations and in addition $\sim 3 \sigma$ measurements of two PK parameters.

3 ANALYSIS AND RESULTS

All the combined TOAs, weighted by their individual uncertainties, were analysed with TEMPO, using the DE405 ephemeris of the Jet Propulsion Laboratory (JPL) (Standish 1998, 2004) and the ELL1 (Lange et al. 2001) binary model. TEMPO minimizes the sum of the weighted squared timing residuals, producing a set of improved pulsar parameters and the post-fit timing residuals. The uncertainties on the TOAs from each telescope are scaled by an appropriate factor to achieve a uniform reduced $\chi^2 \simeq 1$ for each data set. The best post-fitting timing solution of all the combined residuals is presented in Fig. 1. In the top panel, the post-fit versus time is shown, with arbitrary offsets of the different data sets, where it is clear that the uncertainties of most of the data points are comparable. By comparing the parameters we get by different combinations of data sets (i.e. only the 1400 MHz data or without Jodrell), we concluded that it is much more efficient to finally use all the available data sets together, as shown in the lower panel of Fig. 1.

3.1 Timing parallax and distance

Apart from the common method of DM distance estimation (~ 410 pc) and the more rare optical one ($d = 840 \pm 90$ pc) for PSR J1012+5307, there is another way of measuring the distance to a pulsar, with pulsar timing. In general, the timing residuals of nearby pulsars demonstrate an annual parallax. This timing parallax is obtained by measuring a time delay of the TOAs caused by the curvature of the emitted wavefronts at different positions of the Earth in its orbit. This time delay has an amplitude of $r_{E\odot}^2 \cos \beta / (2cd)$ (Lorimer & Kramer 2005), where $r_{E\odot}$ is the Earth–Sun distance, β the ecliptic latitude of the pulsar, c the speed of light and d the distance to the pulsar. This effect has been measured for very few pulsars like PSR B1855+09 (Kaspi, Taylor & Ryba 1994), PSR J1713+0747 (Camilo, Foster & Wolszczan 1994), PSR J0437–4715 (Sandhu et al. 1997), PSR J1744–1134 (Toscano et al. 1999), PSR J2145–0750 (Löhmer et al. 2004) and PSR J0030+0451 (Lommen et al. 2006). Here for the first time, we measure a parallax $\pi = 1.2 \pm 0.3$ mas for PSR J1012+5307. This parallax corresponds to a distance of $d = 822 \pm 178$ pc which is consistent with the $d = 840 \pm 90$ pc measured from the optical observations. The difference with the DM distance may point to a sparse free electron distribution in this location of the Galaxy (Gaensler et al. 2008; Chatterjee et al. 2009). By combining the optical and timing parallax distance measurements we calculate the weighted mean (Wall & Jenkins 2003) of the distance getting an improved value of $d = 836 \pm 80$ pc.

² <http://www.atnf.csiro.au/research/pulsar/tempo/>

Table 2. Timing parameters for PSR J1012+5307. Comparison between the data sets from EPTA, Effelsberg until 2008 and Effelsberg until 2001 (Lange et al. 2001).

Parameters	EPTA	Effelsberg 2008	Effelsberg 2001
Right ascension, α (J2000)	10 ^h 12 ^m 33 ^s .4341010(99)	10 ^h 12 ^m 33 ^s .434089(13)	10 ^h 12 ^m 33 ^s .43364(3)
Declination, δ (J2000)	53°07′02″.60070(13)	53°07′02″.6001(2)	53°07′02″.5878(4)
μ_α (mas yr ⁻¹)	2.562(14)	2.56(2)	2.62(13)
μ_δ (mas yr ⁻¹)	-25.61(2)	-25.49(2)	-25.0(2)
Parallax, π (mas)	1.22(26)	0.8(3)	<1.6
ν (Hz)	190.2678376220576(5)	190.2678376220611(8)	190.267837621910(3)
$\dot{\nu}$ (s ⁻²)	-6.20063(3) × 10 ⁻¹⁶	-6.20077(5) × 10 ⁻¹⁶	-6.2070(5) × 10 ⁻¹⁶
P (ms)	5.255749014115410(15)	5.25574901411531(2)	0.00525574901411947(7)
\dot{P} (s s ⁻¹)	1.712794(9) × 10 ⁻²⁰	1.712833(13) × 10 ⁻²⁰	1.71456(15) × 10 ⁻²⁰
Epoch (MJD)	50700.0	50700.0	50700.0
DM (cm ⁻³ pc)	9.02314(7)	9.0209(3)	9.022(3)
Orbital period, P_b (d)	0.60467271355(3)	0.60467271355(4)	0.6046727133(2)
Projected semimajor axis, x (lt-s)	0.5818172(2)	0.5818175(2)	0.5818174(5)
η ($\equiv e \sin \omega$)	1.2(3) × 10 ⁻⁶	1.6(3) × 10 ⁻⁶	1.1(5) × 10 ⁻⁶
κ ($\equiv e \cos \omega$)	0.06(31) × 10 ⁻⁶	0.14(34) × 10 ⁻⁶	0.20(50) × 10 ⁻⁶
Eccentricity, e^*	1.2(3) × 10 ⁻⁶	1.6(3) × 10 ⁻⁶	1.1(5) × 10 ⁻⁶
Longitude of the periastron, ω (°) *	93(14)	85(12)	79(24)
T_{ASC} (MJD)	50700.08162891(4)	50700.08162891(5)	50700.08162905(9)
\dot{P}_b (s s ⁻¹)	5.0(1.4) × 10 ⁻¹⁴	4(2) × 10 ⁻¹⁴	0.3(3) × 10 ⁻¹²
\dot{x} (s s ⁻¹)	2.3(8) × 10 ⁻¹⁵	<1.8 × 10 ⁻¹⁵	<1.8 × 10 ⁻¹⁵
Solar system ephemeris model	DE405	DE405	DE200
Number of TOAs	2892	1972	1213
rms timing residual (μ s)	3.1	2.7	3.1

*The eccentricity and the longitude of the periastron are calculated from the Laplace–Lagrange parameters, η and κ . Figures in parentheses are the nominal 1σ TEMPO uncertainties in the least-significant digits quoted.

3.2 Improved 3D velocity measurement and Galactic motion

Combining the proper motion measured from timing (Table 2) and the distance to the system and the radial velocity of $v_r = 44 \pm 8 \text{ km}^{-1} \text{ s}$ from the optical observations of the WD, Lange et al. (2001) managed to determine the full 3D motion of the pulsar relative to the SSB. Our new timing results improve the proper motion measurements by an order of magnitude and using the combined parallax and optical distance we recalculate the 3D motion of the pulsar. We derive transverse velocities of

$$v_\alpha = \mu_\alpha d = 10.2 \pm 1.0 \text{ km s}^{-1}, \quad (1)$$

and

$$v_\delta = \mu_\delta d = 101.5 \pm 9.7 \text{ km s}^{-1}. \quad (2)$$

This yields a total transverse velocity of $v_t = 102.0 \pm 9.8 \text{ km s}^{-1}$. Using the radial velocity from the optical measurements, we get the space velocity of the system $v_{\text{space}} = 111.4 \pm 9.5 \text{ km s}^{-1}$, consistent and almost three times more precise than the previous value. In addition, this value is still consistent with the average space velocity of millisecond pulsars of 130 km s^{-1} (Lyne et al. 1998; Toscano et al. 1999).

Since we know the 3D velocity of PSR J1012+5307, we can try, for the first time, to track its Galactic path in time and space. Assuming a characteristic age of ~ 10 Gyr and applying a model for the Galactic potential (Kuijken & Gilmore 1989; Paczyński 1990), we derive the evolutionary path of PSR J1012+5307 in the Galaxy from the point it started emitting as a millisecond pulsar. In the top part of Fig. 2, the projection of the evolutionary path of the pulsar on the Galactic plane is shown, where the arrow indicates the current position of the pulsar and the star indicates the position of

the Sun, for the Kuijken & Gilmore (1989) model (Paczyński 1990 derives similar results). It is obvious that the pulsar is presently at one of its closest approaches to the Sun, which is why we can actually observe it. PSR J1012+5307 reaches maximum distances of ~ 30 kpc through its path, spending only a small fraction of its lifetime close to the Solar system orbit. In Fig. 2 (bottom), the movement of PSR J1012+5307 above and below the Galactic plane is shown versus time indicating that the pulsar is oscillating with a period of ~ 0.6 Gyr reaching a maximum distance of ~ 7 kpc above and below the Galactic plane.

3.3 Eccentricity

PSR J1012+5307 is a low eccentricity binary system. In our current timing solution, we measure a value for the eccentricity of $(1.2 \pm 0.3) \times 10^{-6}$. However, as shown in Lange et al. (2001), the Shapiro delay cannot be separated from the Roemer delay for this system, which leads to a small correction to this eccentricity value and specifically to the first Laplace–Lagrange parameter $\eta = e \sin \omega$. Thus, following their convention, for a companion mass of $m_c = 0.16(2) M_\odot$, a mass ratio $q = 10.5(5)$ and a mass function of $f_m = 0.000578 M_\odot$, we derive the range r and shape s of the Shapiro delay according to

$$r = 4.9255 (m_c/M_\odot) \mu\text{s}, \quad (3)$$

and

$$s = \sin i = \left[\frac{f_m(q+1)^2}{m_c} \right]^{1/3}. \quad (4)$$

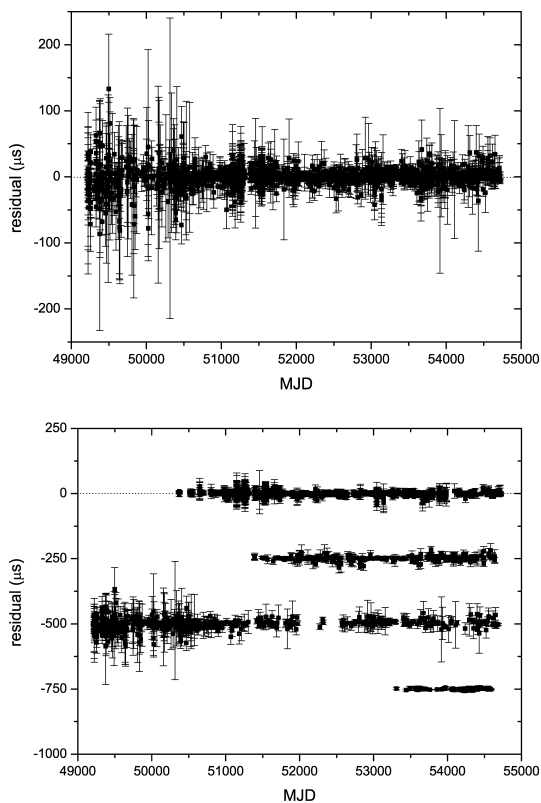


Figure 1. Top: post-fit timing residuals for the data set of each telescope. From top to bottom, Effelsberg, Westerbork, Jodrell and Nançay. Bottom: post-fit timing residuals. Best-timing solution with all the data sets yields the parameters in Table 2.

The intrinsic value of η , calculated from equation (A22) of Lange et al. (2001), due to the contribution of the Shapiro delay, is $\eta = (-1.4 \pm 3.4) \times 10^{-7}$. The true eccentricity of the system is $e = \sqrt{\eta^2 + \kappa^2}$, where $\kappa = \text{ecos } \omega = (0.6 \pm 3.1) \times 10^{-7}$. By solving this equation in a Monte Carlo simulation (Fig. 3), for data sets of the values and uncertainties of the intrinsic η and κ , we obtain an upper limit for the intrinsic eccentricity:

$$e < 5.2 \times 10^{-7} \quad (68 \text{ per cent CL}), \quad (5)$$

$$e < 8.4 \times 10^{-7} \quad (95 \text{ per cent CL}). \quad (6)$$

This limit is better than the previously published value (Lange et al. 2001).

This improved limit has another significant importance. Using the fluctuation-dissipation theorem, Phinney (1992) predicted that the orbital eccentricity, of a pulsar-WD binary system is correlated with the orbital period. Specifically, there is the theoretical prediction of a relic orbital eccentricity due to convective eddy currents in the mass accretion process of the neutron star from the companion while in the red giant phase. In Lange et al. (2001), the eccentricity limit of PSR J1012+5307 was plotted versus the orbital period and was compared with the model curves of the Phinney & Kulkarni (1994) model. Our current eccentricity limit is much lower than the one in Lange et al. (2001), but still in good agreement with the predictions from this model.

3.4 Changes in the projected semimajor axis

A change in the projected semimajor axis has been measured in the current analysis, for the first time, for PSR 1012+5307. The

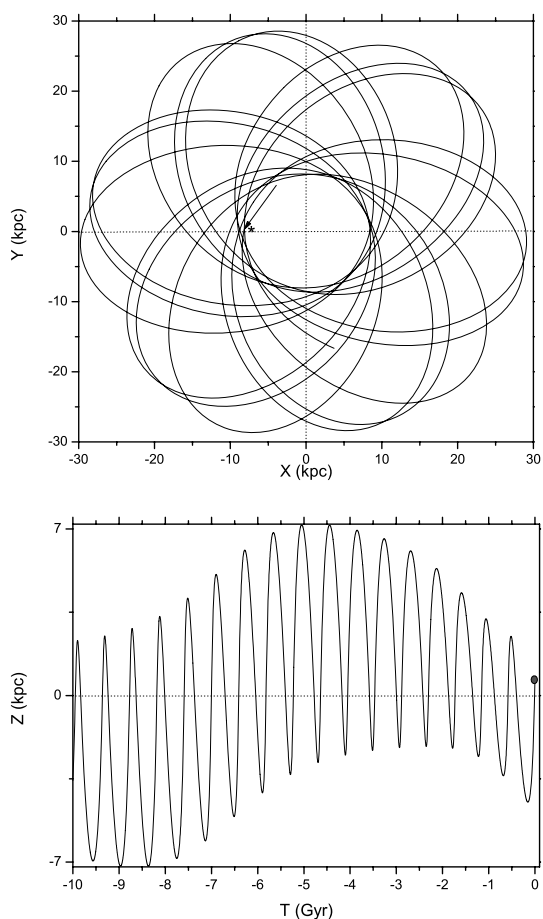


Figure 2. Top: evolutionary path of PSR J1012+5307 on the Galactic plane. With arrow the current position of the pulsar and with * the position of the Sun is noted. Bottom: the oscillations of PSR J1012+5307 above and below the Galactic plane through time.

observed value of $\dot{x}_{\text{obs}} = 2.3(8) \times 10^{-15}$ can be the result of the various effects (Lorimer & Kramer 2005),

$$\dot{x}_{\text{obs}} = \dot{x}^{\text{D}} + \dot{x}^{\text{GW}} + \frac{d\epsilon_A}{dt} + \dot{x}^{\text{m}} + \dot{x}^{\text{SO}} + \dot{x}^{\text{planet}} + \dot{x}^{\text{PM}}. \quad (7)$$

The first term, \dot{x}^{D} , is the Doppler correction, which is the combined effect of the proper motion of the system (Shklovskii 1970) and a correction term for the Galactic acceleration. The contribution for the Galactic acceleration, \dot{x}^{Gal} , is of order 6×10^{-20} . Furthermore, we calculate the contribution of the Shklovskii effect to be $\dot{x}^{\text{Shk}} = x(\mu_\alpha^2 + \mu_\delta^2)d/c \sim 8 \times 10^{-19}$. Both the contributions are very small compared to the observed value, thus, this term can be neglected.

The second term, \dot{x}^{GW} is arising from the shrinking of the orbit due to gravitational-wave damping,

$$\dot{x}^{\text{GW}} = -x \frac{64}{5} \left(\frac{2\pi}{P_b} \right)^{8/3} \frac{(T_\odot m_c)^{5/3} q}{(q+1)^{1/3}} = (-8.2 \pm 1.7) \times 10^{-20} \quad (8)$$

(Peters 1964), where $T_\odot = GM_\odot/c^3 = 4.9255 \mu\text{s}$ and m_c is expressed in units of solar masses. x is the projected semimajor axis and P_b the orbital period. This contribution again is much smaller than the current measurement precision.

The third term, $d\epsilon_A/dt$, is the contribution of the varying aberration caused by geodetic precession of the pulsar spin axis, and is typically of order $\Omega^{\text{geod}} P/P_b \approx 2 \times 10^{-18}$ (Damour & Taylor

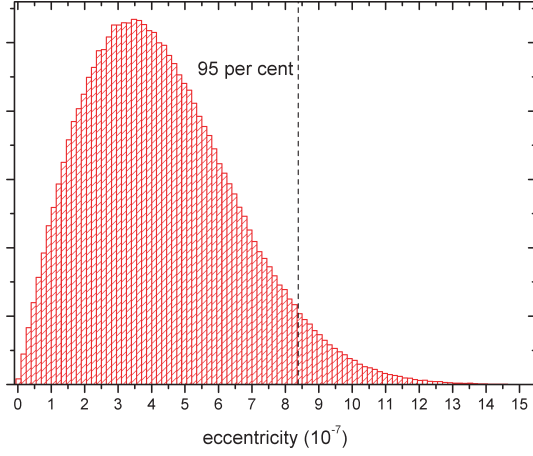


Figure 3. Distribution of values for the intrinsic eccentricity from Monte Carlo simulations. The dashed line cuts the distribution at the 95 per cent of the values.

1992). For a recycled pulsar, like PSR J1012+5307, the spin is expected to be close to parallel to the orbital angular momentum, which further suppresses this effect. Hence, the contribution is at least three orders of magnitude smaller than the observed.

The fourth term, \dot{x}^m , is representing a change in the size of the orbit caused by mass loss from the binary system. We investigate the mass loss due to the loss of rotation energy by the pulsar, which we consider as the dominant mass-loss effect. We initially calculate the change in the orbital period from the same contribution as follows:

$$\dot{P}_b^m = 8\pi^2 \frac{I_p}{c^2 M} \frac{\dot{P}}{P^3} P_b \sim 10^{-16}, \quad (9)$$

where $M = m_p + m_c$ and the moment of inertia of the pulsar $I_p \sim 10^{45} \text{ g cm}^2$. Subsequently, by Kepler's third law, we calculate the change in the projected semimajor axis of the orbit to be $\sim 10^{-17}$. Thus, we can also neglect this contribution.

The fifth and the sixth terms, \dot{x}^{SO} and \dot{x}^{planet} , are the contributions due to the classical spin-orbit coupling caused by a spin-induced quadrupole moment of the companion and the existence of an additional planetary companion, respectively. They can both be neglected. For the first one to be significant, a main-sequence star or a rapidly rotating WD companion (Wex et al. 1998; Kaspi et al. 2000) would be necessary. The second is not being considered because there is no evidence for another companion to the pulsar.

Since all the other contributions are much smaller than the observed variation of the projected semimajor axis, we conclude that the measured value is arising from the last term of equation (7), \dot{x}^{PM} . This is a variation of x caused by a change of the orbital inclination while the binary system is moving relatively to the SSB (Arzoumanian et al. 1996; Kopeikin 1996; Sandhu et al. 1997). The measurement of the effect is presented in the following equation:

$$\dot{x}^{\text{PM}} = 1.54 \times 10^{-16} x \cot i (-\mu_\alpha \sin \Omega + \mu_\delta \cos \Omega), \quad (10)$$

where Ω is the position angle of the ascending node. The quantities x , μ_α and μ_δ are expressed in s and mas yr^{-1} , respectively. The proper motions and the inclination angle have been measured and since we measure the value of $\dot{x}^{\text{PM}} = \dot{x}_{\text{obs}}$, we can, for the first time, restrict the orbital orientation Ω of PSR J1012+5307. In Fig. 4, the \dot{x}^{PM} versus the position angle of the ascending node is presented. Unfortunately, our measured value cannot fully restrict the orientation, however from the lower limits of \dot{x}_{obs} we derive

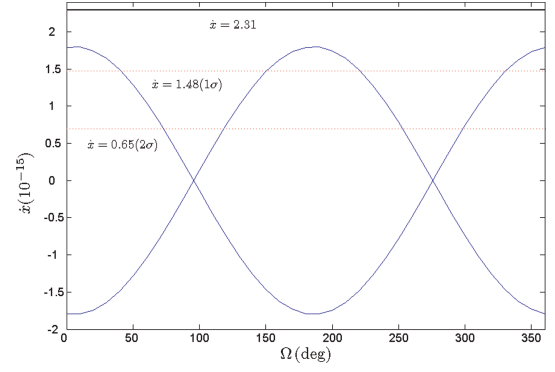


Figure 4. Change of the projected semimajor axis versus position angle of the ascending node. The two curves have been produced for $i = 52^\circ$ (peak at 180°) and $i = 128^\circ$ (peak at 0°). The solid line represents the measured value of \dot{x} and the dashed lines the 1σ and 2σ limits of \dot{x} , from top to bottom. The latter constrains the orientation Ω .

significant limits for the position angle. For an inclination angle of $i = 52^\circ$, we get

$$151^\circ < \Omega < 220^\circ \quad (68 \text{ per cent CL}), \quad (11)$$

and

$$117^\circ < \Omega < 255^\circ \quad (95 \text{ per cent CL}), \quad (12)$$

while for $i = 128^\circ$

$$\Omega < 40^\circ \quad \& \quad \Omega > 331^\circ \quad (68 \text{ per cent CL}), \quad (13)$$

and

$$\Omega < 74^\circ \quad \& \quad \Omega > 297^\circ \quad (95 \text{ per cent CL}). \quad (14)$$

3.5 Orbital period variations

There are several effects that can contribute to changes in the observed orbital period of a binary system that can be either intrinsic to the orbit or just kinematic effects. The most important terms are

$$\dot{P}_b = \dot{P}_b^m + \dot{P}_b^T + \dot{P}_b^D + \dot{P}_b^{\text{GW}} + \dot{P}_b^{\text{G}}. \quad (15)$$

\dot{P}_b , measured here for the first time $\dot{P}_b = 5.0(1.4) \times 10^{-14}$, is the observable rate of change of the orbital period. The first and second terms, \dot{P}_b^m , \dot{P}_b^T , are the contributions from the mass loss from the binary and from tidal torques, respectively. They can both be neglected in the case of PSR J1012+5307 because the first one is very small, as shown before ($\sim 10^{-16}$), and the second is also small due to the lack of interaction between the pulsar and the companion.

The third term, \dot{P}_b^D , is identical to the first term of equation (7). In order to account for the Galactic acceleration, we have extended the Damour & Taylor (1991) expression (for a flat rotation curve) to high Galactic latitudes

$$\left(\frac{\dot{P}_b}{P_b}\right)^{\text{Gal}} = -\frac{K_z | \sin b |}{c} - \frac{\Omega_\odot^2 R_\odot}{c} \left(\cos l + \frac{\beta}{\beta^2 + \sin^2 l} \right) \cos b, \quad (16)$$

where $\beta \equiv (d/R_\odot) \cos b - \cos l$. K_z is the vertical component of Galactic acceleration taken from Holmberg & Flynn (2004), which for Galactic heights $z \equiv |d \sin b| \leq 1.5 \text{ kpc}$ can be approximated with sufficient accuracy by

$$K_z (10^{-9} \text{ cm s}^{-2}) \simeq 2.27 z_{\text{kpc}} + 3.68(1 - e^{-4.31 z_{\text{kpc}}}), \quad (17)$$

where $z_{\text{kpc}} \equiv z(\text{kpc})$. $R_{\odot} = 8.0 \pm 0.4$ (Eisenhauer et al. 2003) and $\Omega_{\odot} = 27.2 \pm 0.9 \text{ km s}^{-1} \text{ kpc}^{-1}$ (Feast & Whitelock 1997) are the Sun's Galactocentric distance and Galactic angular velocity ($= \text{Oort's } A - B$). For the pulsar's Galactic coordinates of $l = 160.3$ and $b = 50.9$, we find

$$\dot{P}_{\text{b}}^{\text{Gal}} = (-5.6 \pm 0.2) \times 10^{-15}. \quad (18)$$

We also calculate the contribution due to the Shklovskii effect according to the following:

$$\dot{P}_{\text{b}}^{\text{Shk}} = \frac{(\mu_{\alpha}^2 + \mu_{\delta}^2) d}{c} P_{\text{b}} = (7.0 \pm 0.7) \times 10^{-14}, \quad (19)$$

where we used the measured proper motion and the weighted mean of the distance discussed earlier, d . So, by summing we yield the Doppler correction,

$$\dot{P}_{\text{b}}^{\text{D}} = \dot{P}_{\text{b}}^{\text{Gal}} + \dot{P}_{\text{b}}^{\text{Shk}} = (6.4 \pm 0.7) \times 10^{-14}. \quad (20)$$

The fourth term, $\dot{P}_{\text{b}}^{\text{GW}}$, is the contribution due to gravitational wave emission. In general relativity, for circular orbits it is given by

$$\dot{P}_{\text{b}}^{\text{GW}} = \dot{P}_{\text{b}}^{\text{GR}} = -\frac{192\pi}{5} \left(\frac{2\pi}{P_{\text{b}}} \right)^{5/3} \frac{(T_{\odot} m_{\text{c}})^{5/3} q}{(q+1)^{1/3}}. \quad (21)$$

For PSR J1012+5307, we find $\dot{P}_{\text{b}}^{\text{GW}} = (-1.1 \pm 0.2) \times 10^{-14}$.

All the previous terms are the ones that are expected to contribute by using general relativity (GR) as our theory of gravity. However, most alternative theories of gravity predict an extra contribution to the observed orbital period variation, via dipole radiation (see Will 1993, 2001 and references therein). This dipolar gravitational radiation results from the difference in gravitational binding energy of the two bodies of a binary system, and is expected to be much larger than the quadrupolar contribution, especially if the binding energies of the two bodies of the binary system differ significantly. Thus, the case of PSR J1012+5307, where there is a pulsar-WD system, is ideal for testing the strength of such emission. One finds for small-eccentricity systems

$$\dot{P}_{\text{b}}^{\text{dipole}} = -4\pi^2 \frac{T_{\odot} \mu}{P_{\text{b}}} \kappa_{\text{D}} \mathcal{S}^2, \quad (22)$$

where m_{c} is expressed in units of solar masses. κ_{D} refers to the dipole self-gravitational contribution, which takes different values for different theories of gravity (zero for GR) and $\mathcal{S} = s_{\text{p}} - s_{\text{c}}$ is the difference in the 'sensitivities' of the two bodies (see Will (1993) for definition), and μ is the reduced mass, $m_{\text{p}} m_{\text{c}} / M$, of the system. The sensitivity of a body is related to its gravitational self-energy ε . In the post-Newtonian limit $s \simeq \varepsilon / mc^2$, which gives $\sim 10^{-4}$ for a WD (Will 2001). Hence, we can neglect s_{c} in equation (22) since $s_{\text{p}} \sim 0.2$. Using the mass ratio q , equation (22) can be written as

$$\dot{P}_{\text{b}}^{\text{dipole}} = -4\pi^2 \frac{T_{\odot} m_{\text{c}}}{P_{\text{b}}} \frac{q}{q+1} \kappa_{\text{D}} s_{\text{p}}^2. \quad (23)$$

For a specific theory of gravity, κ_{D} is known and s_{p} can be calculated as a function of the equation of state of neutron star matter.

Finally, there are theories that predict that the locally measured gravitational constant G changes with time as the Universe expands. A changing gravitational constant would cause a change in the orbital period, which for neutron star-WD systems can be written as

$$\dot{P}_{\text{b}}^{\dot{G}} = -2 \frac{\dot{G}}{G} \left[1 - \left(1 + \frac{m_{\text{c}}}{2M} \right) s_{\text{p}} \right] P_{\text{b}} \quad (24)$$

(Damour, Gibbons & Taylor 1988; Nordtvedt 1990).

The intrinsic change of the orbital period is the observed value minus the Doppler correction term from equation (20),

$$\dot{P}_{\text{b}}^{\text{intr}} = \dot{P}_{\text{b}} - \dot{P}_{\text{b}}^{\text{D}} = (-1.5 \pm 1.5) \times 10^{-14}, \quad (25)$$

which agrees well with the GR prediction given above as

$$\dot{P}_{\text{b}}^{\text{exc}} = \dot{P}_{\text{b}}^{\text{intr}} - \dot{P}_{\text{b}}^{\text{GR}} = (-0.4 \pm 1.6) \times 10^{-14}. \quad (26)$$

Hence, there is no need for a $\dot{P}_{\text{b}}^{\text{dipole}}$ or $\dot{P}_{\text{b}}^{\dot{G}}$ to explain the observed variation of the orbital period. On the other hand, this can be used to set limits for a wide class of alternative theories of gravity, which we will show in the following sections.

3.6 A generic limit for dipole radiation

A tight system comprising a strongly self-gravitating neutron star and a weakly self-gravitating WD should be a very efficient emitter of gravitational dipole radiation, if there is any deviation from general relativity that leads to a non-vanishing κ_{D} in equation (22). Hence, observations of such systems are ideal to constrain deviations of that kind. PSR J1012+5307 turns out to be a particularly useful system to conduct such a test, since: (1) the WD nature of the companion is affirmed optically; (2) the mass estimates in this double-line system are free of any explicit strong-field effects,³ which are a priori unknown, if we do not want to restrict our analysis to specific theories of gravity; (3) the estimated mass of the pulsar seems to be rather high, which is important in the case of strong field effects that occur only above a certain critical mass, like the spontaneous scalarization (Damour & Esposito-Farese 1993).

In the previous section, we have shown that the change in the orbital period is in full agreement with the prediction by general relativity, once the kinematic contributions are accounted for. Hence, any deviations from general relativity leading to a different $\dot{P}_{\text{b}}^{\text{GW}}$ is either small or compensated for a potential $\dot{P}_{\text{b}}^{\dot{G}}$. However, we can already limit the variation of the gravitational constant by using the published limit of $\dot{G}/G = (4 \pm 9) \times 10^{-13} \text{ yr}^{-1}$ from the Lunar Laser Ranging (LLR) (Williams, Turyshev & Boggs 2004). In combination with equation (24) it gives $\dot{P}_{\text{b}}^{\dot{G}} = (-1 \pm 3) \times 10^{-15}$, for the most conservative assumption $s_{\text{p}} = 0$. Hence, $\dot{P}_{\text{b}}^{\text{dipole}} = (-0.2 \pm 1.6) \times 10^{-14}$, which with the help of equation (23) converts into

$$\kappa_{\text{D}} s_{\text{p}}^2 = (0.5 \pm 6.0) \times 10^{-5} \quad (95 \text{ per cent CL}). \quad (27)$$

Furthermore, if we assume $s_{\text{p}} = 0.1(m_{\text{p}}/M_{\odot})$ (c.f. Damour & Esposito-Farese 1992) we find

$$\kappa_{\text{D}} = (0.2 \pm 2.4) \times 10^{-3} \quad (95 \text{ per cent CL}). \quad (28)$$

This number improves upon the previously published limit for PSR J1012+5307 (Lange et al. 2001) by more than an order of magnitude.

For the tensor-scalar theories of Damour & Esposito-Farese (1996) $\kappa_{\text{D}} \mathcal{S}^2 \simeq (\alpha_{\text{p}} - \alpha_{\text{c}})^2 \simeq (\alpha_{\text{p}} - \alpha_0)^2 < 6 \times 10^{-5}$, assuming that the effective coupling strength of the companion WD to the scalar field, α_{c} , is much smaller than the pulsars and is approximately α_0 , where α_0 is a reference value of the coupling at infinity. This value improves slightly on the previously published limit of 7×10^{-5} (Nice et al. 2005), obtained from PSR J0751+1807. If the non-linear coupling parameter β_0 is of order 10 or larger, then neutron

³ The mass estimation for the weakly self-gravitating WD companion is done with Newtonian gravity (Callanan et al. 1998), and in any Lorentz-invariant theory of gravity the theoretical prediction for the mass ratio does not contain any explicit strong-field-gravity effects (Damour 2007).

stars are much more weakly coupled to the scalar field than WDs (Esposito-Farese 2005). In this case, for PSR J1012+5307, $(\alpha_p - \alpha_c)^2 \approx \alpha_0 < 6 \times 10^{-5}$, which is an order of magnitude weaker than the limit 3.4×10^{-6} from PSR J1141–6545 (Bhat, Bailes & Verbiest 2008). Actually, in tensor–scalar theories of gravity, the latter is possibly the most constraining pulsar binary system. However, since there has been no optical identification of the companion, that could establish its WD nature without mass determination based on a specific gravity theory, it is not yet possible to derive a general theory independent limit for dipole radiation from PSR J1141–6545, as done here with PSR J1012+5307.

In the future, more accurate determination of the distance and improvement of our \dot{P}_b value could further increase the precision of the PSR J1012+5307 limit.

3.7 Combined limits on \dot{G} and the dipole radiation with millisecond pulsars

In the previous section, we have used the LLR limit for \dot{G} in order to provide a test for dipole radiation with a single binary pulsar system. On the other hand, a generic test for \dot{G} cannot be done with a single binary pulsar, since in general theories that predict a variation of the gravitational constant typically also predict the existence of dipole radiation (Will 1993).⁴ From equations (22) and (24), we can see that $\dot{P}_b^{\dot{G}} \propto P_b$, whereas $\dot{P}_b^{\text{dipole}} \propto P_b^{-1}$. Hence, one can combine any two binary pulsars, with tight limits for \dot{P}_b and different orbital periods, in a joint analysis to break this degeneracy, and to provide a test for \dot{G} and the dipole radiation that is based purely on pulsar data. A formally consistent way of doing this with WD binary pulsars is the application of equation

$$\frac{\dot{P}_b^{\text{exc}}}{P_b} = -2 \frac{\dot{G}}{G} \left[1 - \left(1 + \frac{m_c}{2M} \right) s_p \right] - 4\pi^2 \frac{T_{\odot} \mu}{P_b^2} \kappa_D s_p^2 \quad (29)$$

(see equations 24 and 22) to both binary pulsars, and solving in a Monte Carlo simulation this set of two equations for \dot{G}/G and κ_D . This procedure properly accounts for the correlations due to this mutual dependence, and thus provides a self-consistent test for \dot{G} and the dipole radiation, that does not rely on LLR limits or theory specific assumptions. There remains the problem of getting a good estimate for s_p in a general theory independent test. As before, we will use $s_p = 0.1$ (m_p/M_{\odot}) keeping in mind that the limits given below are subject to certain changes, if a different assumption for s_p is made.

With its short orbital period and its fairly well-determined masses PSR J1012+5307 is an ideal candidate for such a combined analysis. Presently, the best binary pulsar limit for \dot{G} comes from PSR J0437–4715 (Deller et al. 2008; Verbiest et al. 2008), where $\dot{P}_b^{\text{dipole}} = 0$ has been used in the analysis to obtain the limit for \dot{G} . Using this pulsar in combination with PSR J1012+5307 in a joint analysis as introduced above gives, with a 95 per cent confidence level (CL),

$$\frac{\dot{G}}{G} = (-0.7 \pm 3.3) \times 10^{-12} \text{ yr}^{-1} = (-0.009 \pm 0.045) H_0, \quad (30)$$

and

$$\kappa_D = (0.3 \pm 2.5) \times 10^{-3}, \quad (31)$$

⁴ It is interesting to point out, that in the Jordan–Fierz–Brans–Dicke theory $\dot{P}_b^{\text{dipole}} + \dot{P}_b^{\dot{G}} = 0$ for binary pulsars with WD companions that have orbital periods ~ 10 d.

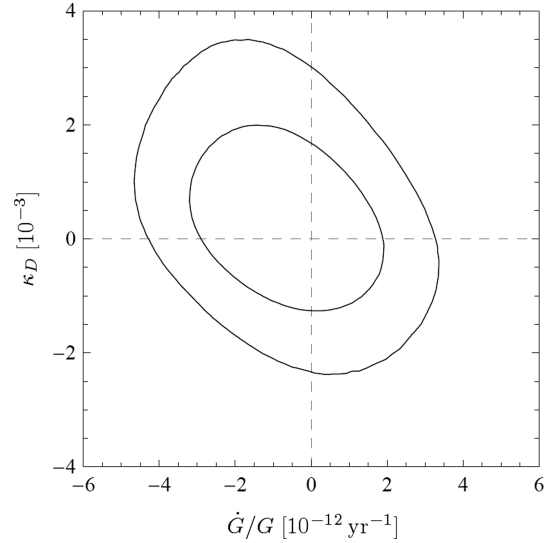


Figure 5. Contour plots of the one and 2σ confidence regions on \dot{G}/G and κ_D jointly. The elongation of the regions reflects the correlation due to the mutual dependence of the two systems, PSR J1012+5307 and PSR J0437–4715, in this combined test.

where $H_0 = 74 \text{ km s}^{-1} \text{ Mpc}^{-1}$ has been used as a value for the Hubble constant (Riess et al. 2009). Our pulsar test therefore restricts \dot{G}/G to less than a 20th of the expansion rate of the Universe.

The limit for \dot{G} given here is clearly weaker than the one given in Deller et al. (2008). The main reason for this is that the equation for $\dot{P}_b^{\dot{G}}$ used by Deller et al. (2008) does not account for the sensitivity of the pulsar as in equation (24). Furthermore, the combined analysis still allows for a certain range for $\dot{P}_b^{\text{dipole}}$ in PSR J0437–4715, leading to a somewhat weaker limit compared with an analysis that uses $\dot{P}_b^{\text{dipole}} = 0$, as can be seen in Fig. 5. Although this limit for \dot{G} is weaker than the LLR limit, it still provides a useful independent addition to the LLR result, as has been argued in Verbiest et al. (2008). We performed the same analysis using PSR J1713+0747 (Splaver et al. 2005) instead of PSR J0437–4715 and this produced a 20 per cent weaker limit for the gravitational constant variation.

The limit for the dipole radiation is slightly weaker than the one given in the previous section. However, in contrast to the limit of the previous section, the limit here does not rely on the LLR result for \dot{G} , and therefore constitutes an independent test based solely on binary pulsar observations.

We would like to stress two facts about the advantage of combining specifically these two binary pulsars. First, in both cases, the companion WD is identified optically, and its non-compact nature is ascertained independently of the underlying theory of gravity. Secondly, the two pulsars seem to be rather heavy and similar in mass ($\sim 1.7 M_{\odot}$),⁵ which is important in case we have effects like spontaneous scalarization above a critical neutron star mass (Damour & Esposito-Farese 1993). In the future, more accurate measurements of \dot{P}_b and distance of the two pulsars could constrain even more our derived limits.

⁵ In general, PSR J0437–4715 does not allow the determination of the pulsar mass, since this requires the mass function, which contains explicit strong-field contributions. Within the generic class of conservative gravity theories (Damour & Taylor 1992; Will 1993), for instance, only the effective gravitational mass, $\mathcal{G}m_p$, of PSR J0437–4715 can be determined. However, if one assumes that G deviates less than 20 per cent from G , the pulsar mass is in the range of 1.5–2.0 solar masses.

4 CONCLUSIONS

We have presented results from the high-precision timing analysis of 15 yr of EPTA data for PSR J1012+5307. A first ever measurement of the timing parallax $\pi = 1.2(3)$ and distance has been obtained for this pulsar. Combined with information from optical observations of the WD companion an improved 3D velocity has been derived for the system. This information enables the derivation of the complete evolutionary path of the pulsar in the Galaxy, showing that it spent most of its lifetime far away from the Solar system orbit. In addition, an improved limit on the extremely low intrinsic eccentricity, $e < 8.4 \times 10^{-7}$ (95 per cent CL), has been acquired, which agrees well with the theoretical eccentricity-orbital period relation (Phinney & Kulkarni 1994).

Of particular interest is the measurement of the variation of the projected semimajor axis, $\dot{x} = 2.3(8) \times 10^{-15}$ which is caused by a change in the orbital inclination as the system moves relative to the SSB. This measurement allowed us to set limits on the positional angle of the ascending node, for the first time, the last unknown parameter in fully describing the orientation of this binary system.

As a result of the significant measurement of the change in the orbital period of the system, $5.0(1.4) \times 10^{-14}$, and the identified nature of the two bodies in this binary system, tests for alternative gravity theories could be performed. First, a stringent, generic limit for the dipole radiation has been obtained from PSR J1012+5307, $\kappa_{\text{D}} s_{\text{p}}^2 = 0.5 \pm 6.0 \times 10^{-5}$ (95 per cent CL), with the use of the \dot{G} limit from LLR. Secondly, in a self-consistent analysis we have used PSR J1012+5307 together with PSR J0437–4715 to derive a combined limit on the dipole radiation and the variation of the gravitational constant, $\kappa_{\text{D}} = (0.4 \pm 2.6) \times 10^{-3}$ and $\dot{G}/G = (-0.7 \pm 3.3) \times 10^{-12} \text{ yr}^{-1}$ (95 per cent CL) respectively. These limits have been derived just with the use of millisecond pulsar-WD binaries and are valid for a wide class of alternative theories of gravity.

ACKNOWLEDGMENTS

We are very grateful to all staff at the Effelsberg, Westerbork, Jodrell Bank and Nançay radio telescopes for their help with the observations. Kosmas Lazaridis was supported for this research through a stipend from the International Max Planck Research School (IMPRS) for Astronomy and Astrophysics at the Universities of Bonn and Cologne. We are grateful to Paulo Freire for valuable discussions.

REFERENCES

Arzoumanian Z., Joshi K., Rasio F. A., Thorsett S. E., 1996, in Johnston S., Walker M. A., Bailes M., eds, ASP Conf. Ser. Vol. 105, Pulsars: Problems and Progress, IAU Colloq. 160. Astron. Soc. Pac., San Francisco. p. 525
 Backer D. C., Dexter M. R., Zepka A., D. N., Wertheimer D. J., Ray P. S., Foster R. S., 1997, PASP, 109, 61
 Bhat N. D. R., Bailes M., Verbiest J. P. W., 2008, Phys. Rev. D, 77, 124017
 Callanan P. J., Garnavich P. M., Koester D., 1998, MNRAS, 298, 207
 Camilo F., Foster R. S., Wolszczan A., 1994, ApJ, 437, L39
 Chatterjee S. et al., 2009, ApJ, 698, 250
 Cordes J. M., Lazio T. J. W., 2002, preprint (astro-ph/0207156)
 Damour T., 2007, preprint (arXiv:0704.0749)
 Damour T., Esposito-Farèse G., 1992, Class. Quantum Grav., 9, 2093
 Damour T., Esposito-Farèse G., 1993, Phys. Rev. Lett., 70, 2220
 Damour T., Esposito-Farèse G., 1996, Phys. Rev. D, 54, 1474
 Damour T., Taylor J. H., 1991, ApJ, 366, 501

Damour T., Taylor J. H., 1992, Phys. Rev. D, 45, 1840
 Damour T., Gibbons G. W., Taylor J. H., 1988, Phys. Rev. Lett., 61, 1151
 Deller A. T., Verbiest J. P. W., Tingay S. J., Bailes M., 2008, ApJ, 685, L67
 Driebe T., Schoenberner D., Bloeker T., Herwig F., 1998, A&A, 339, 123
 Eisenhauer F., Schödel R., Genzel R., Ott T., Tecza M., Abuter R., Eckart A., Alexander T., 2003, ApJ, 597, L121
 Ergma E., Sarna M. J., Gerskevits-Antipova J., 2001, MNRAS, 321, 71
 Esposito-Farèse G., 2005, in Novello M., Perez Bergliaffa S., Ruffini R., eds, The Tenth Marcel Grossmann Meeting: On Recent Developments in Theoretical and Experimental General Relativity, Gravitation and Relativistic Field Theories. World Scientific, Singapore, p. 647
 Feast M., Whitelock P., 1997, MNRAS, 291, 683
 Gaensler B. M., Madsen G. J., Chatterjee S., Mao S. A., 2008, Publ. Astron. Soc. Aust., 25, 184
 Holmberg J., Flynn C., 2004, MNRAS, 352, 440
 Janssen G. H., Stappers B. W., Kramer M., Nice D. J., Jessner A., Cognard I., Purver M. B., 2008, A&A, 490, 753
 Kaspi V. M., Taylor J. H., Ryba M., 1994, ApJ, 428, 713
 Kaspi V. M., Lackey J. R., Mattox J., Manchester R. N., Bailes M., Pace R., 2000, ApJ, 528, 445
 Kopeikin S. M., 1996, ApJ, 467, L93
 Kramer M., Xilouris K. M., Lorimer D. R., Doroshenko O., Jessner A., Wielebinski R., Wolszczan A., Camilo F., 1998, ApJ, 501, 270
 Kramer M., Lange C., Lorimer D. R., Backer D. C., Xilouris K. M., Jessner A., Wielebinski R., 1999, ApJ, 526, 957
 Kuijken K., Gilmore G., 1989, MNRAS, 239, 571
 Lange C., Camilo F., Wex N., Kramer M., Backer D., Lyne A., Doroshenko O., 2001, MNRAS, 326, 274
 Löhmer O., Kramer M., Driebe T., Jessner A., Mitra D., Lyne A. G., 2004, A&A, 426, 631
 Lommen A. N., Kipporn R. A., Nice D. J., Splaver E. M., Stairs I. H., Backer D. C., 2006, ApJ, 642, 1012
 Lorimer D. R., Kramer M., 2005, Handbook of Pulsar Astronomy. Cambridge Univ. Press, Cambridge
 Lorimer D. R., Lyne A. G., Festin L., Nicastro L., 1995, Nat, 376, 393
 Lyne A. G. et al., 1998, MNRAS, 295, 743
 Nicastro L., Lyne A. G., Lorimer D. R., Harrison P. A., Bailes M., Skidmore B. D., 1995, MNRAS, 273, L68
 Nice D. J., Splaver E. M., Stairs I. H., Löhmer O., Jessner A., Kramer M., Cordes J. M., 2005, ApJ, 634, 1242
 Nordtvedt K., 1990, Phys. Rev. Lett., 65, 953
 Paczyński B., 1990, ApJ, 348, 485
 Peters P. C., 1964, Phys. Rev. Lett., 136, 1224
 Phinney E. S., 1992, Phil. Trans. Roy. Soc. A, 341, 39
 Phinney E. S., Kulkarni S. R., 1994, ARA&A, 32, 591
 Riess A. G. et al., 2009, ApJ, 699, 539
 Sandhu J. S., Bailes M., Manchester R. N., Navarro J., Kulkarni S. R., Anderson S. B., 1997, ApJ, 478, L95
 Shklovskii I. S., 1970, SvA, 13, 562
 Splaver E. M., Nice D. J., Stairs I. H., Lommen A. N., Backer D. C., 2005, ApJ, 620, 405
 Standish E. M., 1998, JPL Planetary and Lunar Ephemerides, DE405/LE405, Memo IOM 312.F-98-048. JPL, Pasadena
 Standish E. M., 2004, A&A, 417, 1165
 Toscano M., Sandhu J. S., Bailes M., Manchester R. N., Britton M. C., Kulkarni S. R., Anderson S. B., Stappers B. W., 1999, MNRAS, 307, 925
 Verbiest J. P. W. et al., 2008, ApJ, 679, 675
 Voûte J. L. L., Kouwenhoven M. L. A., van Haren P. C., Langerak J. J., Stappers B. W., Driesens D., Ramachandran R., Beijerd T. D., 2002, A&A, 385, 733
 Wall J. V., Jenkins C. R., 2003, Practical Statistics for Astronomers. Cambridge Univ. Press, Cambridge

Wex N., Johnston S., Manchester R. N., Lyne A. G., Stappers B. W., Bailes M., 1998, MNRAS, 298, 997
Will C., 2001, Living Rev. Relativ., 4, 1
Will C. M., 1993, Theory and Experiment in Gravitational Physics. Cambridge Univ. Press, Cambridge

Williams J. G., Turyshev S. G., Boggs D. H., 2004, Phys. Rev. Lett., 93, 261101

This paper has been typeset from a \TeX/L\TeX file prepared by the author.